



ELSEVIER

Available online at [www.sciencedirect.com](http://www.sciencedirect.com)

SCIENCE @ DIRECT®

Nuclear Instruments and Methods in Physics Research B 202 (2003) 1–7

**NIM B**  
Beam Interactions  
with Materials & Atoms

[www.elsevier.com/locate/nimb](http://www.elsevier.com/locate/nimb)

# Finding possible transition states of defects in silicon-carbide and alpha-iron using the dimer method

Fei Gao <sup>a,\*</sup>, Graeme Henkelman <sup>b</sup>, William J. Weber <sup>a</sup>, L. Rene Corrales <sup>a</sup>, Hannes Jónsson <sup>b</sup>

<sup>a</sup> *Fundamental Science Directorate, Pacific Northwest National Laboratory, MS K8-93, P.O. Box 999, Richland, WA 99352, USA*

<sup>b</sup> *Department of Chemistry, Box 351700, University of Washington, Seattle, WA 98195-1700, USA*

## Abstract

Energetic primary recoil atoms from ion implantation or fast neutron irradiation produce isolated point defects and clusters of both vacancies and interstitials. The migration energies and mechanisms for these defects are crucial to successful multiscale modeling of microstructural evolution during ion-implantation, thermal annealing, or under irradiation over long periods of time. The dimer method is employed to search for possible transition states of interstitials and small interstitial clusters in SiC and  $\alpha$ -Fe. The method uses only the first derivatives of the potential energy to find saddle points without knowledge of the final state of the transition. In SiC, the possible migration pathway for the C interstitial is found to consist of the first neighbor jump via a Si site or second neighbor jump, but the relative probability for the second neighbor jump is very low. In  $\alpha$ -Fe, the possible transition states are studied as a function of interstitial cluster size, and the lowest energy barriers correspond to defect migration along  $\langle 111 \rangle$  directions. However, this paper addresses whether migrating interstitial clusters can thermally change their direction, and the activation energies and corresponding mechanisms for changing the direction of these clusters are determined.

© 2002 Elsevier Science B.V. All rights reserved.

PACS: 71.15.D; 61.72; 66.30.L; 82.20.D

Keywords: Dimer method; Defects and defect clusters; Defect migration; Transition states; SiC and Fe

## 1. Introduction

Molecular dynamics (MD) has emerged as the main computational tool for modeling irradiation effects in materials, and it has been broadly applied in recent years to the study of primary damage

formation in metals [1–3], wide-band-gap semiconductors [4,5] and oxides [6,7]. These simulations provide a good understanding of defect production, defect clustering, and the arrangements and properties of self-interstitial atoms and vacancies in cascades. The point defects and clusters created in cascades have important consequences for microstructure evolution under cascade damage conditions, and understanding their stability, mobility and interaction with microstructures is crucial for successfully modeling long-time microstructure

\* Corresponding author. Tel.: +1-509-376-6275; fax: +1-509-376-5106.

E-mail address: [fei.gao@pnl.gov](mailto:fei.gao@pnl.gov) (F. Gao).

evolution under irradiation. Consequently, the motion of interstitial clusters in various transition metals [8–10] has been investigated using MD methods. The interstitial clusters in metals have very high mobility, with activation energies between 0.022 and 0.03 eV. Only small interstitial clusters (<4) are observed to change their glide direction during the time frame of MD simulations (~5 ns), but the directional change for larger clusters is inaccessible to MD due to simulation time constraints. In the case of SiC, little is known about point defect migration.

In order to overcome the ‘time barrier’ in MD simulation, the so-called hyperdynamics method has been developed by Voter [11,12]. This method has been employed to study infrequent events, such as the diffusive motion of adatoms and clusters on a surface, but it remains to be seen if this method can be successfully applied to defect migration and microstructure evolution under irradiation. Another method for finding saddle points, without knowledge of the final state of transition, is the ‘dimer’ method that has been recently developed by Henkelman and Jónsson [13]. In this paper, the dimer method is employed to search for the possible transition states of interstitials and small interstitial clusters in SiC and  $\alpha$ -Fe. In addition to the calculation of point defect and cluster migration along the  $\langle 111 \rangle$  direction in  $\alpha$ -Fe, the directional change of interstitial clusters is investigated.

## 2. Dimer method

The dimer method has been described in detail elsewhere [13], so only the central principles are provided here. The dimer method involves working with two atomic images of the system. Two images are displaced a small distance  $\Delta R$  from the common midpoint  $\vec{R}$ :

$$\vec{R}_i = \vec{R} \pm \Delta R \vec{N} \quad (i = 1, 2), \quad (1)$$

where the vector  $\vec{N}$ , which is a unit vector, defines the dimer orientation. When a transition state search is launched from an initial configuration, a random unit vector can be assigned to  $\vec{N}$ . Fig. 1(a) shows the two images, various positions and force vectors of the dimer. The energy,  $E_0$ , and the force

acting on the midpoint of the dimer,  $\vec{F}_R$ , as well as the curvature of the potential  $C$  along the dimer, can be calculated from the energies and the forces ( $E_1$ ,  $\vec{F}_1$ ,  $E_2$  and  $\vec{F}_2$ ) acting on the two images:

$$E_0 = \frac{E}{2} + \frac{\Delta R}{4} (\vec{F}_1 - \vec{F}_2) \cdot \vec{N}, \quad (2)$$

$$\vec{F}_R = (\vec{F}_1 + \vec{F}_2)/2 \quad (3)$$

and

$$C = \frac{(\vec{F}_2 - \vec{F}_1) \cdot \vec{N}}{2\Delta R} = \frac{E - 2E_0}{(\Delta R)^2}, \quad (4)$$

where  $E$  is the energy of the dimer.

To search a saddle point involves two operations, namely rotating and translating the dimer. Each time the dimer is displaced, it is necessary to rotate the dimer towards the minimum energy (e.g. minimizing the dimer energy,  $E$ ), which is equivalent to finding the lowest curvature mode at the midpoint  $\vec{R}$  (see Eq. (4)). If  $\vec{\Theta}$ , perpendicular to  $\vec{N}$ , is denoted as the rotational direction within the plane of rotation, the rotational force can be calculated by

$$\vec{F} = (\vec{F}_1^\perp - \vec{F}_2^\perp) * \vec{\Theta} / \Delta R. \quad (5)$$

The key to implementing the rotation scheme of the dimer is to calculate the rotational angle,  $\Delta\theta$ , which brings the force  $\vec{F}$  to zero. Given a small angle of rotation,  $d\theta$ , images 1 and 2 move from  $\vec{R}_1$  and  $\vec{R}_2$  to  $\vec{R}_1^*$  and  $\vec{R}_2^*$ , respectively, from which the new forces  $\vec{F}_1^*$ ,  $\vec{F}_2^*$ ,  $\vec{F}^* = \vec{F}_1^* - \vec{F}_2^*$  and rotational direction  $\vec{\Theta}^*$  can be computed. A finite difference approximation to the change in rotational force,  $F$ , as the dimer rotates through the small angle  $d\theta$  is then given by

$$F' = \frac{\partial F}{\partial \theta} \approx \left| \frac{\vec{F}^* \cdot \vec{\Theta}^* - \vec{F} \cdot \vec{\Theta}}{d\theta} \right|. \quad (6)$$

Within the quadratic approximation of a Taylor expansion of the potential,  $U$ , it is possible to obtain an analytical form of the scalar rotational force on the dimer and its first derivative. These are given by

$$F = A \sin[2(\theta - \theta')] \quad (7)$$

and

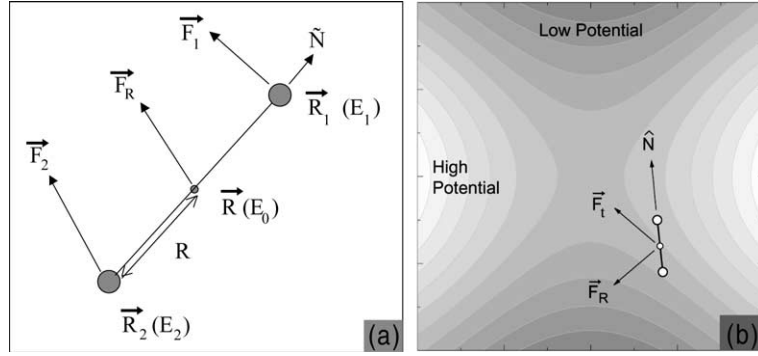


Fig. 1. (a) Schematic illustration of the various positions and force vectors for a dimer, where  $\vec{F}_R$  is an average force acting on the midpoint of the dimer. (b) After the dimer orients itself along the lowest curvature mode, the effective force,  $\vec{F}^+$  for the translation of the dimer is the true force  $\vec{F}_R$  with the component along  $\tilde{N}$  inverted, as defined in Eq. (10). The effective force points towards the nearby saddle point.

$$F' = dF/d\theta = 2A \cos[2(\theta - \theta')], \quad (8)$$

where  $A$  is a constant associated with the curvature of the potential. If  $\theta = 0$  is taken as the initial point in the simulation, then the angle required to bring  $F$  to zero can be obtained from Eqs. (7) and (8) and is given by

$$\Delta\theta = \theta' = -\frac{1}{2} \arctan\left(\frac{2F}{F'}\right). \quad (9)$$

Because the energy of the dimer is minimized by rotation, the dimer will orient itself along the lowest curvature mode. A saddle point search is to find a maximum along the lowest curvature mode, but a minimum along all other modes. In addition to rotation, the dimer needs to be translated and moved up the potential surface. The net translation force acting on the midpoint of the dimer,  $\vec{F}_R$  in Eq. (3), tends to pull the dimer towards a minimum. A modified force,  $\vec{F}^t$ , which brings the dimer to a saddle point is given by

$$\vec{F}^t = \begin{cases} -\vec{F}^{\parallel} & C > 0, \\ \vec{F}_R - 2\vec{F}^{\parallel} & C < 0. \end{cases} \quad (10)$$

This is illustrated in Fig. 1(b). In the initial calculation, the dimer is minimized along a line defined by the initial force, and it is then moved a small distance along the line to calculate the derivative of the effective force, a similar approach to the rotation algorithm in Eq. (6). Newton's

method is used to estimate the zero in the effective force along the line, and the dimer is then moved to that point. After each translation, the dimer is reoriented and moved along a direction conjugate to the previous line minimization. The potentials used to describe the interactions between atoms in SiC are those developed by Gao and Weber [14] based on the Brenner potential formalism [15].

### 3. Results and discussion

#### 3.1. Defects in SiC

The transition states and mechanisms for migration of interstitials in SiC are studied in a cubic box of 125 unit cells consisting of 1000 atoms with periodic boundary conditions. The lowest energy configuration for the C interstitial, based on the potentials used here, is the  $C^+-C\langle 100 \rangle$  dumbbell at a C site, with a formation energy of 3.04 eV. This minimum state is used as the initial configuration for searching saddle points. A dimer separation,  $\Delta R$ , is set at  $10^{-3}$  Å, and the values of the finite difference steps for rotation and translation are  $d\theta = 10^{-4}$  and  $dR = 10^{-3}$  Å, respectively. A maximum move distance for the dimer is set at 0.1 Å, and the dimer search is stopped when the total force of atoms is less than  $10^{-4}$ . The dimer method is run using 800 randomly chosen initial dimer orientations around the minimum.

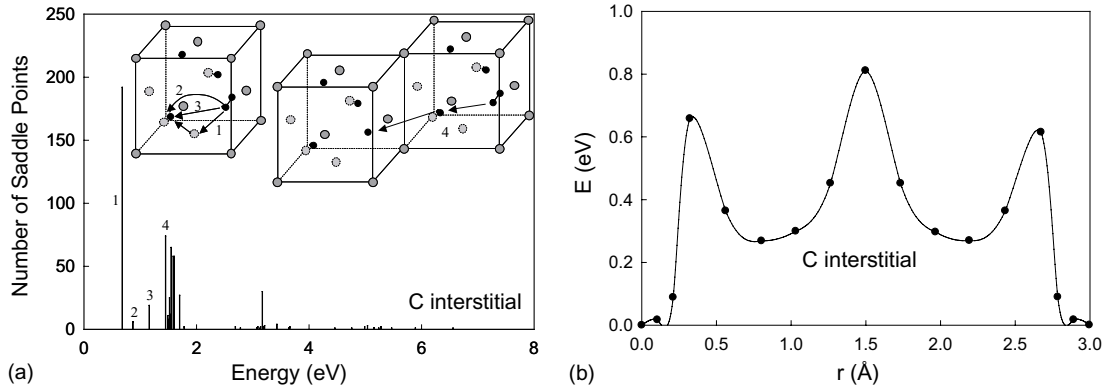


Fig. 2. (a) The results of 800 dimer searches that converge to saddle points associated with the original configuration for a C interstitial in SiC, where the histogram shows how many of the saddle points are in the given energy range. The atomic plots illustrate the possible migration paths of the C interstitial corresponding to the dimer searches. (b) The minimum path for C interstitial calculated using the nudged-elastic band method.

Fig. 2(a) summarizes the results of 800 dimer searches for a C dumbbell interstitial, where 623 searches converge to saddle points below 6 eV. Four searches fail to converge within the imposed limit of 500 iterations. Although 173 searches converge to saddle points, they are not associated with the original minimum configuration, which are excluded in Fig. 2(a). The saddle points with energy less than 1.8 eV attract 70% of the 800 dimer searches, and only 8% of the dimer searches are distributed in the range from 2 to 6 eV. The corresponding mechanisms of the four events indicated by transition numbers are also illustrated in Fig. 2(a). The first mechanism represents the lowest energy path for a C interstitial with the activation energy of 0.66 eV, in which the C interstitial migrates to the nearest neighbor Si site, forming a  $C^+-Si(100)$  dumbbell, and then migrates to another C site. The second and third mechanisms involve jumps from a C site to other (second nearest neighbor) C sites. The transitions with saddle point energies ranging from 1.5 to 1.70 eV correspond to the movements of several atoms to transport a C interstitial to the fifth nearest neighbor positions, similar to the behavior for pathway 4. Above 1.7 eV there are a large number of different processes, particularly at an energy of 3.17 eV, that involve a group shift of three atoms (including the C interstitial) from their minimum energy positions.

It should be noted that the energies in Fig. 2(a) are not the highest energy barriers for interstitial migration because there are multiple saddle points along a migration pathway. In order to show this, the nudged-elastic band method [16] has been used to calculate the minimum energy path of a  $C^+-C(100)$  interstitial, and the results, which correspond to pathway 1, are shown in Fig. 2(b). It can be seen that there are three significant saddle points along the path with the energies of 0.66, 0.81 and 0.66 eV, respectively. The lowest energy saddle point in Fig. 2(a) corresponds to the first energy barrier, but the migration energy for the C interstitial is actually 0.81 eV, which is consistent with experimental observations of recovery processes in SiC near room temperature [17]. If all relevant transition states can be obtained, it is possible to simulate defect evolution over long-time scales by combining the dimer method with kinetic Monte Carlo (KMC) [18], the so called long-time-scale dynamics. However, because multiple saddle points can exist along defect migration pathways in SiC, as shown in Fig. 2(b), the long-time-scale dynamics of defect evolution could fail if defects cannot escape from these local minima. The original Tersoff potentials have been tested, and the results show very similar behavior to the potential used here. One of the approaches to overcome this problem may be to use a scheme that smoothes the potential surface, such as the

diffusion equation method (DEM) [19], or develop much better potentials for SiC.

### 3.2. Interstitials and interstitial clusters in $\alpha$ -Fe

Supercells containing from 2000 to 8192 atoms are employed to ensure that the effects of interactions of a cluster with its periodic images are negligible. The  $\langle 110 \rangle$  dumbbell is used as an initial configuration for searching saddle points. A summary of the results for a single interstitial is shown in Fig. 3(a). Of the 500 dimer searches, 425 converge to saddle points with an energy of 0.163 eV, which corresponds to the configuration change from a  $\langle 110 \rangle$  dumbbell to a  $\langle 111 \rangle$  crowdion. Fifteen searches converge to other saddle points, but they are not associated with the originally minimum configuration. Sixty searches fail to find saddle points within 500 iterations. The continued searches from the final configuration of previous run (i.e.  $\langle 111 \rangle$  crowdion) result in two significant saddle points, one representing the directional change from the  $\langle 111 \rangle$  crowdion to a  $\langle 110 \rangle$  dumbbell and another one corresponding to an energy barrier for migration along the  $\langle 111 \rangle$  direction. Once the saddle points are determined, it is possible to trace out the minimum energy path using a method described elsewhere [13]. The energy path for a single interstitial is shown in Fig. 3(b), where the relative coordination is used such that the

distance from the  $\langle 110 \rangle$  dumbbell to the final  $\langle 111 \rangle$  configuration is one unit. It can be seen that the migration of a single interstitial consists of two mechanisms. One involves rotation from the stable  $\langle 110 \rangle$  dumbbell to a metastable  $\langle 111 \rangle$  crowdion with an energy of 0.163 eV, and the other is the migration of a crowdion along the  $\langle 111 \rangle$  direction with the activation energy of 0.0022 eV. These mechanisms are similar to those observed in the MD simulations of defect diffusion [8,9].

One of important applications of the dimer method in this paper is to search for the transition states of interstitial clusters. Cluster sizes containing up to 10 SIAs are studied, and all initial states are set as compact  $\langle 111 \rangle$  crowdion cluster configurations. As an example, the results of the dimer searches for a four-member interstitial cluster are summarized in Fig. 4. A total of 603 out of 800 dimer searches converged to saddle points with energies from 0.039 to 3.18 eV. While 102 searches failed to converge within the imposed limit of 500 iterations, 94 searches converged to saddle points that are not associated with the originally minimum configuration. The lowest energy event corresponds to a cluster migration along the  $\langle 111 \rangle$  direction, with an activation energy of 0.039 eV, which is similar to that obtained by MD simulations [8–10]. The second event involves the surface diffusion of atoms, as indicated in the plot, that results in a change in configuration

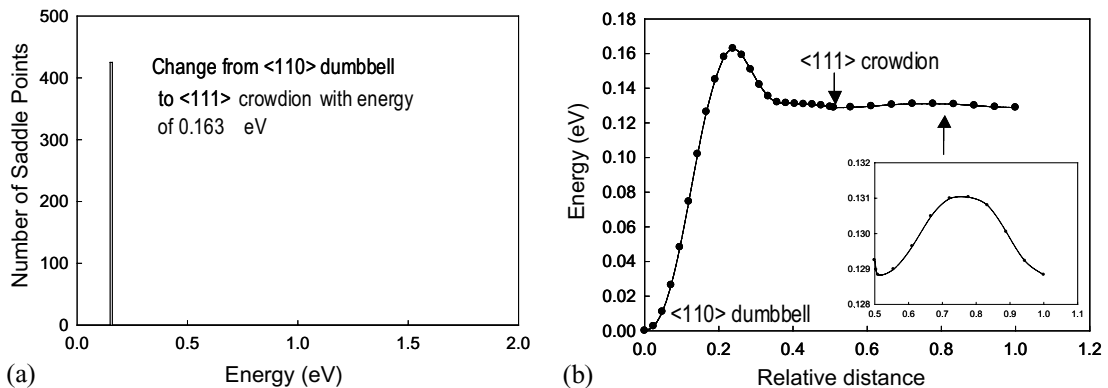


Fig. 3. (a) Saddle points obtained by 500 dimer searches for a single interstitial in  $\alpha$ -Fe that correspond to the directional change from a  $\langle 110 \rangle$  dumbbell to a  $\langle 111 \rangle$  crowdion. (b) The minimum path traced out as the interstitial changes its direction from the initial  $\langle 110 \rangle$  dumbbell to a  $\langle 111 \rangle$  crowdion and migration along the  $\langle 111 \rangle$  direction.

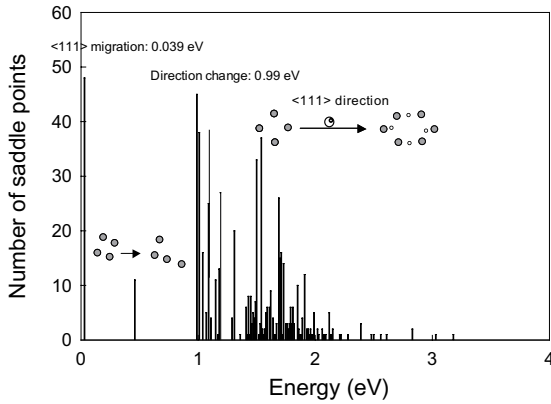


Fig. 4. The results of 800 saddle point searches using the dimer method for a four-member interstitial cluster. The lowest energy event corresponds to cluster migration along the  $\langle 111 \rangle$  direction, but a large number of saddle points with the energies higher than 1 eV were found. These transitions involve the interstitials displaced from their original positions in the  $\langle 111 \rangle$  rows to form a more complex configuration.

from a minimum state to a metastable state. The directional change for a four-member interstitial cluster is found to be the second populated event with an activation energy of 0.99 eV, which is much higher than that for a cluster migrating along  $\langle 111 \rangle$  direction.

The minimum paths associated with the saddle points, which relate to the migration along  $\langle 111 \rangle$  direction and the directional change of clusters, have been traced out for interstitial clusters. It is found that the activation energies for migration along the  $\langle 111 \rangle$  direction vary with cluster size and range from 0.0022 to 0.039 eV, in reasonable agreement with previous studies using MD simulations [10]. The minimum energy paths corresponding to saddle points for directional changes are shown in Fig. 5, where the reaction coordinate is scaled to allow the distance between two minima to be unity. The paths that do not terminate back at zero energy correspond to configuration changes from a  $\langle 110 \rangle$  dumbbell to a  $\langle 111 \rangle$  crowdion for single interstitial and from  $\langle 111 \rangle$  crowdions to  $\langle 110 \rangle$  dumbbells for di- and tri-interstitial clusters. The energy barriers for these processes, which represent the energy for directional change,  $E_{dc}$ , from the  $\langle 111 \rangle$  direction to another, are plotted in Fig. 6, together with the binding energy per defect

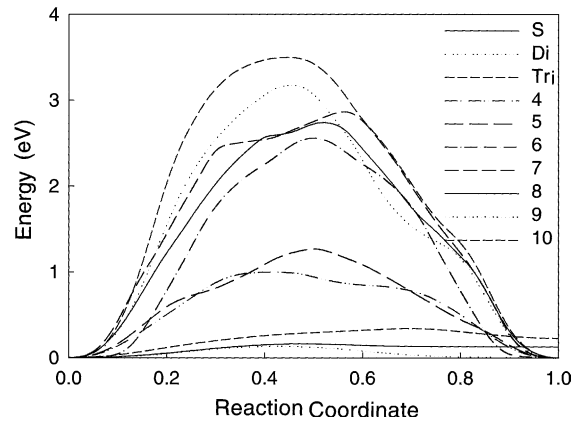


Fig. 5. The minimum paths for the directional change for a cluster size up to 10 SIAs, where the reaction coordinate has been scaled so that 0 represents the initial minimum and 1 indicates the final states.

in a cluster for comparison. As shown, the energy for directional change is very high in comparison with the migration energy along  $\langle 111 \rangle$  direction and generally increases with increasing cluster size. The value for  $E_{dc}$  is 0.163, 0.133 and 0.342 eV for  $N = 1, 2$  and  $3$ , respectively, which are smaller than the migration energy of a single vacancy (0.78 eV for the potential used). These clusters can easily change their direction and be activated at room temperature. The energy of the directional change for a cluster of size 4 and 5 is about 1 eV, and these clusters may change their direction at high tem-

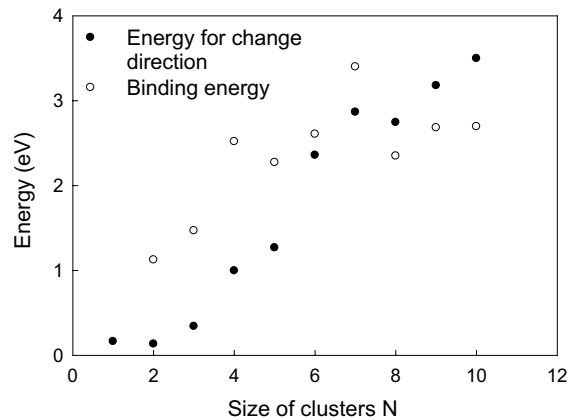


Fig. 6. The energy barriers of the directional change for interstitial clusters in  $\alpha$ -Fe, together with the binding energy per defect in a cluster for comparison.

peratures. When the cluster size is larger than 5,  $E_{dc}$  is in excess of 2 eV, so that the directional change by thermally activated process becomes impossible, even at very high temperatures. It is interesting to note that the binding energy is larger than  $E_{dc}$  for cluster sizes up to seven, above which it is smaller than  $E_{dc}$ . This may suggest that any cluster size larger than seven may not change their direction before they dissociate into small clusters. Detailed analysis shows that single interstitial, di- and tri-interstitial clusters change their direction via  $\langle 110 \rangle$  configurations. When the size of a cluster is larger than three, the situation becomes more complicated, and the mechanism for directional change is completely different from that for small clusters. It is found that the directional change for clusters larger than three is a two-step process, consisting of translation along the  $\langle 100 \rangle$  direction and rotation into an equivalent  $\langle 111 \rangle$  configuration.

#### 4. Summary

The possible transition states of interstitials and their clusters have been studied using the dimer method in SiC and  $\alpha$ -Fe, and the results have been discussed in terms of the development of long-time scale dynamics of defect evolution under irradiation. The possible migration paths for a C interstitial in SiC are found to be a first neighbor jump via a Si site or a second neighbor jump to a C site. Also, the transition states of defects in  $\alpha$ -Fe have been studied as a function of cluster size, and the saddle points generally increase in magnitude with increasing clusters. The migration energies of interstitial clusters along the  $\langle 111 \rangle$  direction range from 0.0022 to 0.039 eV, which is consistent with those obtained using MD simulations. The directional changes for small clusters ( $N = 1, 2$  and  $3$ ) can be thermally activated at room temperature, but clusters of size 4 and 5 may change their direction only at high temperatures. The energy barriers for directional change of a cluster size larger than 5 are in excess of 2 eV so that it is very difficult for them to be activated thermally. Small clusters change their direction via  $\langle 110 \rangle$  dumbbell

mechanism involving rotations into and out of the  $\langle 110 \rangle$  dumbbell configurations, whereas the directional change for larger clusters is a two-step process consisting of a translation along the  $\langle 100 \rangle$  direction and rotation into an equivalent  $\langle 111 \rangle$  configuration.

#### Acknowledgements

This research is supported by the Division of Materials Science and Engineering, Office of Basic Energy Sciences, US Department of Energy under Contract DE-AC06-76RLO 1830.

#### References

- [1] T. Diaz de la Rubia, R.S. Averback, R. Benedek, W.E. King, Phys. Rev. Lett. 59 (1987) 1930.
- [2] D.J. Bacon, A.F. Calder, F. Gao, V.G. Kapinos, S.J. Wooding, Nucl. Instr. and Meth. B 102 (1995) 37.
- [3] D.J. Bacon, F. Gao, Yu.N. Osetsky, J. Nucl. Mater. 276 (2000) 1.
- [4] F. Gao, W.J. Weber, R. Devanathan, Nucl. Instr. and Meth. B 180 (2001) 176.
- [5] K. Nordlund, J. Peltola, J. Nord, J. Keinonen, R.S. Averback, J. Appl. Phys. 90 (2001) 1710.
- [6] B. Park, W.J. Weber, L.R. Corrales, Phys. Rev. B 64 (2001) 174108.
- [7] J.P. Crocombette, D. Ghaleb, J. Nucl. Mater. 295 (2001) 167.
- [8] F. Gao, D.J. Bacon, A.V. Barashev, H.L. Heinisch, Mater. Res. Soc. Symp. Proc. 540 (1999) 703.
- [9] B. Wirth, G.R. Odette, D. Maroudas, G.E. Lucas, J. Nucl. Mater. 224 (1997) 185.
- [10] Yu.N. Osetsky, D.J. Bacon, A. Derra, B.N. Singh, S.I. Golubov, J. Nucl. Mater. 276 (2000) 65.
- [11] A.F. Voter, J. Chem. Phys. 106 (1997) 4665.
- [12] A.F. Voter, Phys. Rev. Lett. 78 (1997) 3908.
- [13] G. Henkelman, H. Jónsson, J. Chem. Phys. 111 (1999) 7010.
- [14] F. Gao, W.J. Weber, Nucl. Instr. and Meth. B 191 (2002) 504.
- [15] D.W. Brenner, Phys. Rev. B 42 (1990) 9458.
- [16] M.R. Sorensen, K.W. Jacobsen, H. Jónsson, Phys. Rev. Lett. 77 (1996) 5067.
- [17] W.J. Weber, W. Jiang, Y. Zhang, A. Hallen, Nucl. Instr. and Meth. B 191 (2002) 514.
- [18] G. Henkelman, H. Jónsson, J. Chem. Phys. 115 (2001) 9657.
- [19] L. Piela, J. Kostrowichi, H. Scheraga, J. Phys. Chem. 93 (1989) 3339.